Journal of
PERIODONTAL RESEARCH

J Periodont Res 2010; 45: 541–549

JOURNAL OF PERIODONTAL RESEARCH
doi:10.1111/j.1600-0765.2010.01269.x

The temporal expression and localization of extracellular matrix metalloproteinase inducer (EMMPRIN) during the development of periodontitis in an animal model

L. Liu[1], C. Li[1,2], X. Cai[3], J. Xiang[1,2], Z. Cao[1,2], W. Dong[2]

[1]Key Laboratory for Oral Biomedical Engineering of Ministry of Education and [2]Department of Periodontology, School and Hospital of Stomatology, Wuhan University, Hongshan District, Wuhan, China and [3]Department of Periodontology, the Affiliated Hospital of Stomatology, School of Medicine, Zhejiang University

Liu L, Li C, Cai X, Xiang J, Cao Z, Dong W. The temporal expression and localization of extracellular matrix metalloproteinase inducer (EMMPRIN) during the development of periodontitis in an animal model. J Periodont Res 2010; 45: 541–549. © 2010 John Wiley & Sons A/S

Background and Objective: We previously demonstrated extracellular matrix metalloproteinase inducer (EMMPRIN) was associated with the matrix metalloproteinases production of human periodontitis. The aim of this study was to investigate the temporal expression and localization of EMMPRIN during ligature-induced periodontitis in rats.

Material and Methods: Periodontitis was inducd in rats by placing a thread around the cervix of the first mandibular molar. Animals were killed 3, 7, 11, 15 or 21 d after ligation. Mandibles were processed for paraffin sections and stained with hematoxylin and eosin or picrosirius red. The distance from the amelocemental junction to the alveolar crest (ACJ–AC) and the area fraction (Area%) of collagen fibers were measured. EMMPRIN was examined by immunohistochemistry and quantified by positive cell counting. Correlation analyses were then performed.

Results: Histologically, alveolar bone was gradually destroyed from day 3 to 11 and then stabilized. Collagen fibers were slightly dissociated on day 3 and extensively broken on day 7. They were reconstructed from day 11 to 21. EMMPRIN was localized predominantly in infiltrating cells and adjacent fibroblasts in interdental gingiva. The number of EMMPRIN-positive cells increased on day 3, peaked on day 7 and then gradually subsided from day 11 to 21. Statistically, there was a moderate positive correlation regarding the ACJ–AC distance ($r = 0.552$, $p < 0.01$) and a strong negative correlation with the Area% of collagen fibers ($r = -0.808$, $p < 0.01$). In gingival epithelium, the immunoreactivity was extremely strong in basal layer cells and sulcular epithelial cells in health. It was greatly enhanced in the inflamed conditions on days 3 and 7. In the interradicular bone, EMMPRIN was localized in the osteoclasts on days 3 and 7, as well as in the osteoblasts from day 11 onwards.

Conclusion: The expression and localization of EMMPRIN are temporally varied during the development of periodontitis. In addition, the inflammation-dependent expression of EMMPRIN might be involved in alveolar bone resorption and collagen breakdown.

Dr Chengzhang Li, MS, PhD, Department of Periodontology, School and Hospital of Stomatology, Wuhan University, 237 Luo Yu Road, Hongshan District, Wuhan 430079, China
Tel: +86 27 8764 6304
Fax: +86 27 8764 6697
e-mail: l56cz@hotmail.com

Key words: extracellular matrix metalloproteinase inducer (EMMPRIN); periodontitis; alveolar bone; extracellular matrix

Accepted for publication November 18, 2009

Periodontitis is a common infectious disease characterized by periodontal tissue destruction, which is mediated by inflammation and involves the loss of alveolar bone and connective tissue, including collagen, proteolycan and other components of the extracellular matrix (1). Matrix metalloproteinases (MMPs) play a key role in the pathogenesis of periodontitis. The breakdown of extracellular matrix is determined by the balance between MMPs and their host-derived endogenous inhibitors (2).

Extracellular matrix metalloproteinase inducer (EMMPRIN) is a type I transmembrane glycoprotein best known as an inducer of MMPs (3). It can stimulate the production of MMP-1, MMP-2, MMP-3, MMP-9, membrane-type 1-MMP (MMP-14) and membrane-type 2-MMP (MMP-15) (3). Other than production of MMPs, it also regulates the chemotaxis of inflammatory cells via interaction with cyclophilin A (4,5). It was previously reported that an increased EMMPRIN level in gingival crevicular fluid was associated with the severity of inflammation in human periodontitis (6). We hypothesized a potential role of EMMPRIN in the extracellular matrix degradation seen in periodontitis (7), and recently demonstrated a correlation between EMMPRIN expression and production of MMPs at the mRNA level in human periodontal disease (8). However, no direct evidence is currently available for the association of EMMPRIN with periodontal tissue destruction. Moreover, as a multifunctional molecule, the overall roles of EMMPRIN in the pathogenesis of periodontitis are still unknown.

The experimental model of ligature-induced periodontitis has been well established for decades. A ligature is able to facilitate plaque accumulation and leads to gingival inflammation, connective tissue breakdown and alveolar bone loss (9,10). Other than inflammation and destruction, resolution and reparative responses are also present in periodontal tissues during the development of experimental periodontitis (11,12). Overall, ligature-induced periodontitis is histologically similar to human periodontitis and can be used to study the pathogenesis of periodontitis. The aim of the present study was to investigate, in an animal model, the association of EMMPRIN with the pathogenesis of periodontitis, by examining the temporal expression and localization of EMMPRIN during ligature-induced periodontitis. We also analyzed the possible correlation of EMMPRIN with alveolar bone loss and collagen breakdown.

Material and methods

Animals

Fifty male 6-wk-old Sprague–Dawley rats (180–230 g body weight) were purchased from the Laboratory Animal Center of Wuhan University. They were housed four or five per cage, with a 12 h–12 h light–dark cycle, temperature of 24 ± 2°C and humidity of 40–60%. The experiment was approved by the Institutional Animal Care and Use Committee of Wuhan University.

Experimental periodontitis

The animals were randomly divided into six groups (days 0, 3, 7, 11, 15 and 21). There were eight rats for each group of days 0, 3, 11, 15 and 21 ($n = 8$) and ten for the group of day 7 ($n = 10$). Rats without ligatures were killed as a healthy control group on day 0. The remaining rats were anesthetized with Su-Mian-Xin, composed of dihydroetorphine hydrochloride, dimethylaniline thiazole, EDTA and haloperidol (0.6 ml/kg body weight, intramuscularly; Veterinary Institute of Military Supplies University, Changchun, China). and a thread (3/0, surgilon, USS/DG, Norwalk, CT, USA) was placed around the cervix of the bilateral first mandibular molars (13). The thread was gently pressed into the gingival sulcus and ligated on the mesial side. The deeper the thread is laid subgingivally, the more damage is caused (9,11); therefore, in order to reduce procedural errors, the thread was placed at almost the same position relative to the gingival margin by the same trained operator. The rats with ligatures were killed by cervical dislocation under anesthesia on days 3, 7, 11, 15 and 21 after ligation for the five groups. Mandibles were harvested and fixed in 4% neutral phosphate buffered formalin for 48 h and decalcified in 10% EDTA solution for 4 wk at 4°C. Bilateral specimens from each rat were respectively processed for mesiodistal and buccolingual paraffin sections (5 μm).

Histological examination and quantification of alveolar bone loss

After deparaffiniziation and rehydration, sections were stained with hematoxylin and eosin for histological examination. Alveolar bone loss was quantified by the distance from the amelocemental junction to the alveolar crest (ACJ–AC), in accordance with our previous histometric distance method (13). The ACJ–AC distance was measured at the distal site of the mandibular first molar on sections using software (Spot Diagnostic Instruments, Sterling Heights, MI, USA). The measurement was performed on three sections for each rat, which were selected from the representative sections at or near the middle site. The site could be recognized by the shape and configuration of tissues. It was a typical rectangular interdental area, including the middle alveolar crest and two bilateral tooth roots, as well as a vault-shaped interradicular region at or near the middle site. All the measurements were carried out by a trained and calibrated examiner who was blind to the groups.

Collagen fiber staining and quantification of collagen breakdown

Collagen fibers were shown by picrosirius red staining according to previously described methods (13,14). In brief, sections were sequentially deparaffinized, rehydrated, stained with 0.1% sirius red F3Ba (Direct Red 80; Fluka, Buchs, Switzerland) for 1 h, washed in acidified water (5 ml acetic acid added to 1 L of distilled water) for 2–3 min, dehydrated and then mounted in resinous medium. The results were observed under a polarization microscope (Olympus BHSP, Tokyo,

Japan). The area fraction (Area%) of collagen fibers in the interdental gingiva was measured in six randomly selected 100 μm × 100 μm fields by Leica Qwin software (Leica Qwin V3, Leica Microsystems, Wetzlar, Germany). Three sections per rat were analysed, and three determinations were averaged for each section.

Immunohistochemistry

Sections were deparaffinized and immersed in methanol with 0.3% hydrogen peroxide for 10 min to inactivate endogenous peroxidase. According to pilot results, treatment to expose epitopes was not necessary. Sections were rinsed in phosphate-buffered saline (3 × 5 min) before being covered with 10% normal rabbit serum for 15 min to block non-specific binding. Next, they were incubated with goat anti-EMMPRIN (1:100 dilution, Abcam, Cambridge, UK) overnight at 4°C. After another rinse, sections were treated with rabbit anti-goat immunoglobulin G for 10 min and then reacted with the avidin–biotin–peroxidase complex for 10 min. Reaction products were visualized by immersing the sections in 0.03% diaminobenzidine solution. Finally, sections were counterstained with hematoxylin. Phosphate-buffered saline was substituted for the primary antibody as a negative control.

To quantify the expression of EMMPRIN, brown-stained cells were counted in nine randomly selected 100 μm × 100 μm areas in the interdental gingiva with a microscope (Olympus Optical Co. Ltd, Tokyo, Japan) under the ×40 objective. Three sections were analyzed for each rat, and nine determinations were summed for each section.

Statistical analyses

The values from the three sections were averaged for each rat. Results are expressed as the mean ± SD for each group. The SPSS statistical package (SPSS Inc., Chicago, IL, USA) was used to analyze the data. The kappa test was used for examiner calibration. Means were compared by analysis of variance (ANOVA) followed by Tukey's test. Bivariate correlation and linear regression were used to analyze the correlation of EMMPRIN expression with the ACJ–AC distance and the Area% of collagen fibers. The null hypothesis was rejected at $p < 0.05$. A value of $|r| > 0.4$ was considered a moderate correlation, while $|r| > 0.7$ was considered a strong correlation.

Results

Histological assessment and quantification of alveolar bone loss

In the interdental area between the first and second molars, epithelial ulceration, vasodilatation and a mild-to-moderate infiltration, predominantly of neutrophils with a few lymphocytes and macrophages, were observed on day 3. Plenty of lymphocytes and macrophages had migrated into the connective tissues by day 7. The inflammatory infiltration was gradually resolved and replaced by reconstructed collagen bundles from day 11 to 21. Osteoclasts were observed on days 3 and 7 in the bone lacuna. The height of the alveolar bone crest was decreased to different degrees in all the ligated groups. Quantitative analyses revealed that the ACJ–AC distance significantly increased in all ligated groups compared with healthy control group (day 0; $p < 0.01$). The ACJ–AC distance increased progressively from day 3 to 11, with a small drop on day 15, and was then slightly aggravated again on day 21. However, there was no significant difference among the groups on days 11, 15 and 21 ($p > 0.01$). In other words, the alveolar bone loss was nearly stable from day 11 to 21. The histological appearances and the quantification of alveolar bone loss in the interdental area are shown in Fig. 1. The kappa test showed good reproducibility for quantitative analyses of the three parameters ($\kappa > 0.75$).

Collagen staining and quantification of collagen breakdown

The collagen bundles were stained yellow, red or green, according to their orientation on a black background, by picrosirius red staining. They were densely and regularly organized in the healthy state (day 0). A few irregular spaces were observed on day 3. The collagen bundles became severely broken on day 7. Newly regenerated collagen bundles emerged on day 11 and grew intensely from day 15 to 21. Briefly, the collagen fibers were destroyed before day 7 and reconstructed from day 11 onwards. Quantitative analyses revealed that the Area% of collagen fibers dropped on day 3 and reached a nadir on day 7. They then increased from day 11 to 21. There was no significant difference between days 0 and 21 ($p > 0.01$). These results are shown in Fig. 2.

Temporal expression and localization of EMMPRIN

Immunohistochemistry revealed that EMMPRIN was widely distributed in the periodontal tissues. Three regions were chosen for observation: the interdental area between the first and second mandibular molars, the gingival epithelium and the interradicular region of the first mandibular molar.

Interdental area— In this area, we focused only on the gingival connective tissue, excluding the alveolar bone and the gingival epithelium. The positive staining was confined to a few cells beneath the epithelium in health on day 0 and enhanced with the inflammatory infiltration on days 3, 7 and 11. The increased expression was mainly localized in infiltrating cells and some adjacent spindle-shape fibroblasts. Based on form, size and location, the immunopositive infiltrating cells could be recognized as mainly lymphocytes and macrophages, as well as a few neutrophils. The immunoreactivity then weakened, and resembled a normal state on days 15 and 21, which was occasionally seen in cells near the sporadically seen abscess.

The number of immunopositive cells was small on day 0, slightly increased on day 3, and peaked because of the severe infiltration on day 7. The cell count subsided on day 11 when the inflammation lessened, but was still higher than in health ($p < 0.01$

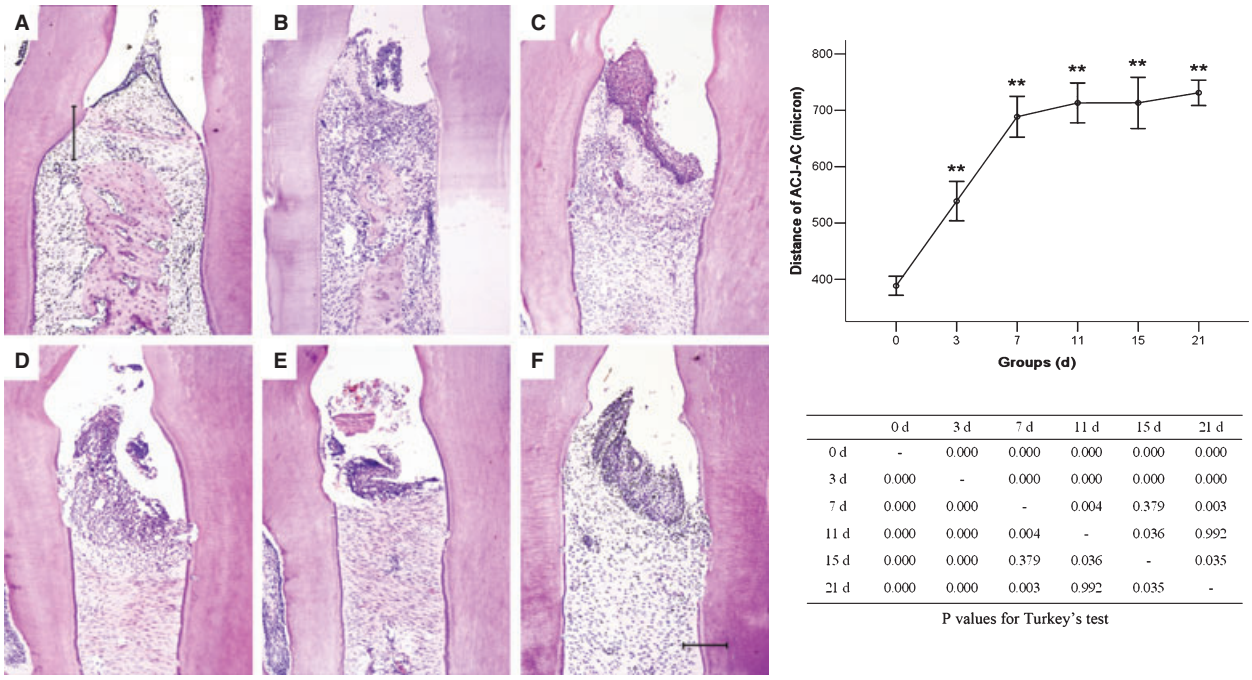

	0 d	3 d	7 d	11 d	15 d	21 d
0 d	-	0.000	0.000	0.000	0.000	0.000
3 d	0.000	-	0.000	0.000	0.000	0.000
7 d	0.000	0.000	-	0.004	0.379	0.003
11 d	0.000	0.000	0.004	-	0.036	0.992
15 d	0.000	0.000	0.379	0.036	-	0.035
21 d	0.000	0.000	0.003	0.992	0.035	-

P values for Turkey's test

Fig. 1. Histological appearances and quantification of alveolar bone loss in the interdental area. The tissue structures were intact on day 0 (A); epithelial ulceration, vasodilatation and inflammatory infiltration were observed on day 3 (B); numerous inflammatory cells migrated into the connective tissues instead of collagen fibers on day 7 (C); some new collagen bundles emerged with the resolution of infiltration on day 11 (D); and more new collagen bundles were formed on days 15 (E) and 21 (F). The longitudinal line in (A) shows the ACJ–AC distance. The quantitative results for alveolar bone loss are shown graphically in the top right-hand panel. Alveolar bone loss was gradually and significantly increased on days 3, 7 and 11 ($p < 0.01$). There were no significant differences among day 11, 15 and 21 ($p > 0.01$). The p-values of pairwise comparison are shown in the table on the bottom right. Scale bar represents 200 μm; $^{**}p < 0.01$ compared with day 0.

compared with day 0). It resembled the healthy level on days 15 and 21 ($p > 0.05$ compared with day 0). This temporal trend was highly coincident with the collagen breakdown from day 0 to 21, and consistent with the loss of alveolar bone before day 11. These results are shown in Fig. 3.

Gingival epithelium— EMMPRIN was distributed in the gingival epithelium in an interesting pattern. The results are described from three aspects: the attached gingival epithelium, the free gingival epithelium and the sulcular epithelium. In health, the positive staining was extremely strong in the basal layer cells and decreased toward the upper layers of the attached gingival epithelium (Fig. 4A,a1). It was mild to moderate in the free gingival epithelium and quite intense in the sulcular epithelium (Fig. 4A,a2). On days 3 and 7, the staining intensity was sharply increased in the attached gingival epithelium (Fig. 4B,b1) with the inflammation of the subepithelial connective tissue. The structures of the free gingival epithelium and the sulcular epithelium were not intact because of ulceration. No significant temporal difference was found in either the attached gingival epithelium or the free gingival epithelium from day 11 to 21, compared with health. There was, however, a marked upsurge in the sulcular epithelium because of cell proliferation (Fig. 4C,c1, c2).

Interradicular region— In the interradicular region, EMMPRIN was weakly expressed by a few cells in health (day 0; Fig. 5A,a). It was considerably increased on days 3 and 7, mainly in the infiltrating cells and large multinuclear osteoclasts in bone lacunas (Fig. 5B,b). Positive staining was frequently observed in numerous square-shaped active osteoblasts lining the bone surface on day 11 (Fig. 5C,c). Then it was occasionally seen on day 15 and rarely visible on day 21.

It is necessary to point out that the histological changes of the alveolar bone were slightly different between the interdental area and the interradicular region. As described above, the interdental alveolar bone was incrementally lost from day 0 to 11 and nearly stabilized from day 11 to 21, whereas the interradicular bone was gradually repaired from day 11 to 21, which was revealed by the increased amount of bone in the interradicular region.

Correlation analyses

The number of EMMPRIN-positive cells showed a strong negative correlation with the Area% of collagen fibers ($r = -0.808$, $p = 0.000$) and a moderate positive correlation with the ACJ–AC distance ($r = 0.552$, $p = 0.002$; Fig. 6). In other words, the temporal expression of EMMPRIN was highly correlated with the collagen breakdown and moderately with the alveolar bone loss.

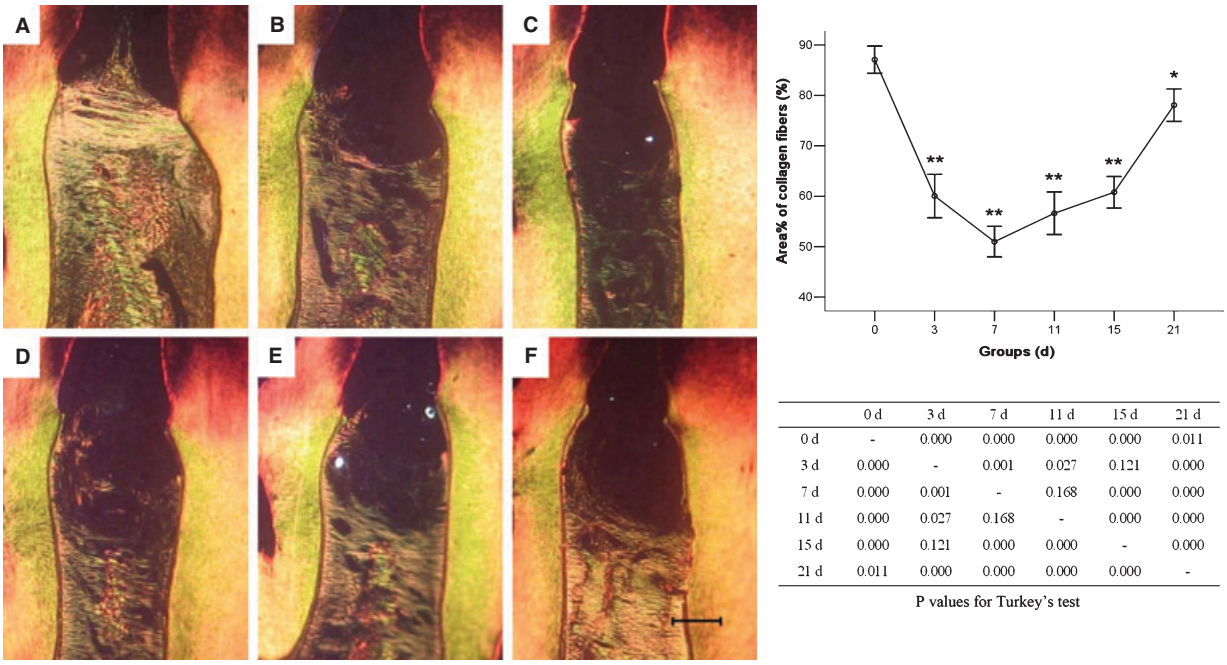

	0 d	3 d	7 d	11 d	15 d	21 d
0 d	-	0.000	0.000	0.000	0.000	0.011
3 d	0.000	-	0.001	0.027	0.121	0.000
7 d	0.000	0.001	-	0.168	0.000	0.000
11 d	0.000	0.027	0.168	-	0.000	0.000
15 d	0.000	0.121	0.000	0.000	-	0.000
21 d	0.011	0.000	0.000	0.000	0.000	-

P values for Turkey's test

Fig. 2. Picrosirius red staining and quantification of collagen breakdown in the interdental area. The collagen bundles are stained yellow, red or green, according to their orientation on a black background. They were correctly organized on day 0 (A); they appeared slightly dissociated with fewer irregular spaces on day 3 (B); they became extensively broken on day 7 (C); a few newly regenerated collagen bundles emerged on day 11 (D); and plenty of reconstructed collagen bundles were observed on days 15 (E) and 21 (F). The quantitative results for collagen breakdown are shown graphically in the top right-hand panel. The Area% of collagen fibers reached a nadir on day 7 and then gradually increased from day 11 to 21. The *p*-values of pairwise comparison are shown in the table on the bottom right. Scale bar represents 200 μm. *$0.01 < p < 0.05$ and **$p < 0.01$ compared with day 0.

Discussion

In this study, we examined the temporal expression and localization of EMMPRIN during the development of ligature-induced periodontitis over a 21 d period. To our knowledge, this is the first study to report the time-dependent changes in the expression and localization of EMMPRIN during periodontitis. We also demonstrated that the inflammation-dependent expression EMMPRIN was correlated with alveolar bone loss and collagen breakdown in the interdental area during periodontitis.

During the 21 d period, inflammation, destruction, resolution and repair were present in the periodontal tissues to different degrees at various stages. These histological characteristics are consistent with the results of previous studies (11–13). EMMPRIN was widely distributed in the rat periodontal tissues and was expressed throughout the 21 d. In the interdental gingiva, the expression of EMMPRIN increased with the aggravation of inflammation and reduced with the resolution of inflammation. This inflammation-dependent expression was in agreement with one of our previous findings that EMMPRIN expression in gingival tissue was associated with the severity of inflammation in human periodontal disease (8). The localization of EMMPRIN in macrophages and lymphocytes was supported by the reports that EMMPRIN was expressed by active T cells (15), macrophages (16) and monocytes (17) *in vitro*. Based on the function of EMMPRIN as a regulator for the chemotaxis of inflammatory cells (3–5), it was speculated that EMMPRIN might contribute to inflammatory infiltration. However, we did not provide formal proof in this study.

The inflammation-dependent expression of EMMPRIN was temporally coincident and statistically correlated with collagen breakdown. It was also partly consistent (before day 11) and moderately correlated with alveolar bone loss. It could therefore be concluded that EMMPRIN, as an inducer of MMPs, might participate in the extracellular matrix degradation of collagen fibers and alveolar bone during periodontitis. EMMPRIN can stimulate MMP-1 production in a mitogen-activated protein kinase p38-dependent manner (18) and MMP-2 expression via activation of A2 and 5-lipoxygenase (19). Nuclear factor-κB was also involved in EMMPRIN-induced intracellular signaling (3,20). In addition, EMMPRIN could be regulated by two cytokines, transforming growth factor-β1 and epidermal growth factor (3,21,22). However, the exact regulatory mechanisms for EMMPRIN-induced production of MMPs during periodontitis are still unknown. Further investigations are needed to elucidate these issues.

Interestingly, EMMPRIN was localized in the osteoclasts during the interradicular bone destruction on days 3 and 7, and also in the osteoblasts during the reparative stages from

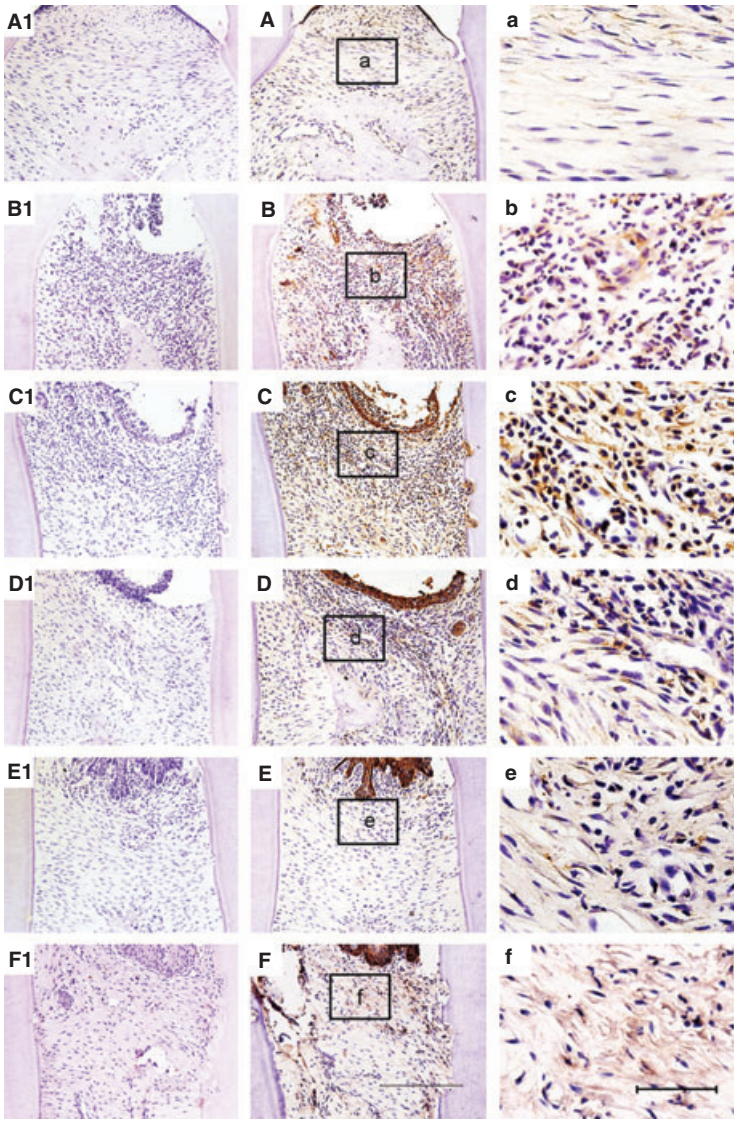

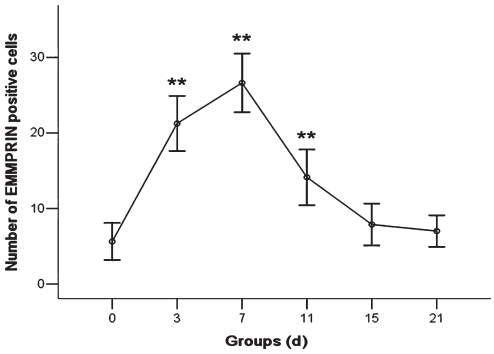

	0 d	3 d	7 d	11 d	15 d	21 d
0 d	-	0.000	0.000	0.000	0.241	0.442
3 d	0.000	-	0.033	0.004	0.000	0.000
7 d	0.000	0.033	0.000	0.000	0.000	0.000
11 d	0.000	0.004	0.000	-	0.000	0.000
15 d	0.241	0.000	0.000	0.000	-	0.684
21 d	0.442	0.000	0.000	0.000	0.684	-

P values for Turkey's test

Fig. 3. Temporal expression and localization of EMMPRIN in the interdental gingiva. EMMPRIN was weakly expressed on day 0 (A,a). It was obviously increased on days 3 (B,b), 7 (C,c) and 11 (D,d) but not on days 15 (E,e) and 21 (F,f). The overexpressed EMMPRIN was mainly localized in infiltrating inflammatory cells and adjacent fibroblasts. Phosphate-buffered saline was substituted for the primary antibody as a negative control and did not stain (A1–F1). The quantitative results for EMMPRIN expression are shown graphically in the top right-hand panel. The number of EMMPRIN-positive cells was increased on day 3, peaked on day 7 and then decreased on day 11, but was still greater than the healthy level ($p < 0.01$). It resembled the healthy level on days 15 and 21 ($p > 0.05$ compared with day 0). The *p*-values of pairwise comparison are shown in the table on the bottom right. Scale bars represent 200 μm in (F) and 50 μm in (f). $^{**}p < 0.01$ compared with day 0.

day 11 to 21, especially in the early stage of repair on day 11. The reparative responses were evidenced by the increased interradicular bone mass. In contrast, alveolar bone repair was not observed in the interdental area to the same degree. We were inclined to believe that the smaller amount of alveolar bone repair was due to greater mechanical stimulion from the ligature or less effective self-cleansing in the interdental area. In any case, the temporal localization of EMMPRIN in both osteoclasts and osteoblasts in different periods indicated that EMMPRIN might be involved in the regulation of alveolar bone remodeling during periodontitis, including resorption and repair.

EMMPRIN could promote osteoclastogenesis by facilitating recruitment of circulating monocytes and macrophages (17,20). It might contribute to alveolar bone resorption by this pathway. Unfortunately, except for a previous report about EMMPRIN expression in the giant cell tumor of bone, scant information is currently available for osteoblast-derived EMMPRIN (20). In fact, alveolar bone is constantly undergoing a remodeling process. In health, there is a balance between the amount of bone resorbed by osteoclasts and the amount of bone formed by osteoblasts (23). In this study, fewer osteoclasts and

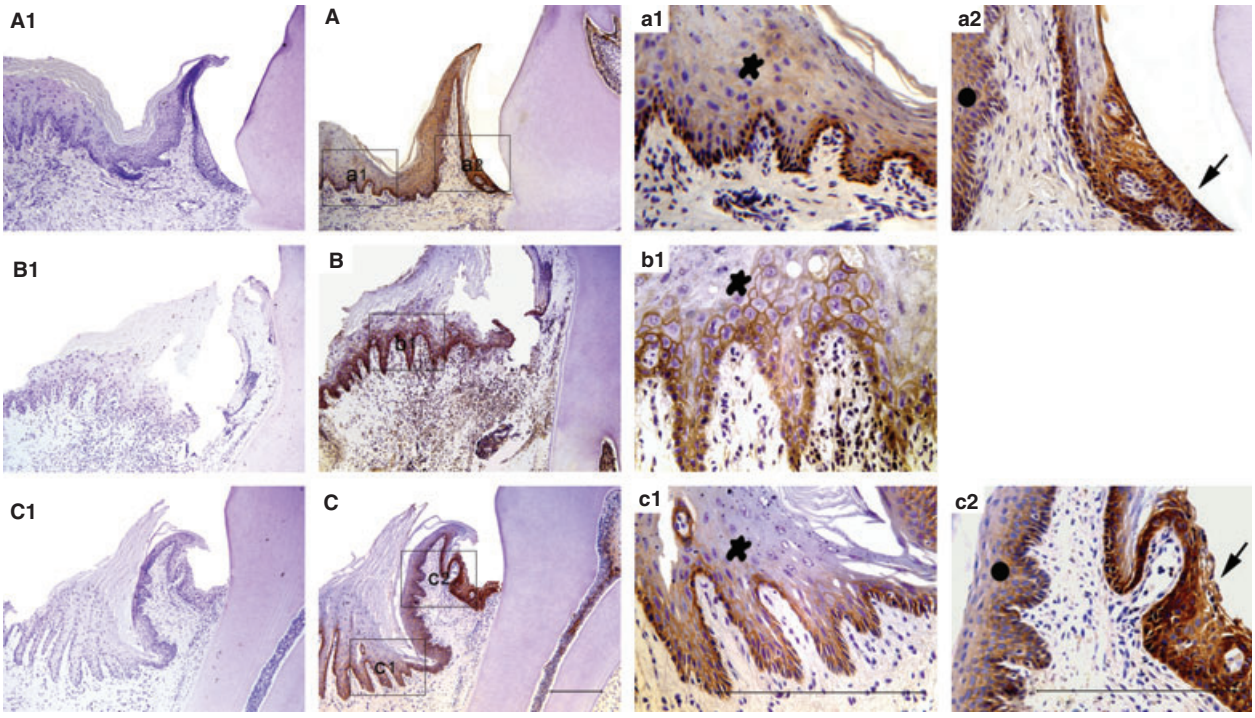

Fig. 4. Temporal expression and localization of EMMPRIN in the gingival epithelium. (A) On day 0 (health), the immunoreactivity was strong in the basal cells, with a decrease toward the upper layers in the attached gingival epithelium (star in a1), mild to moderate immunoreactivity in the free gingival epithelium (filled circle in a2) and intense immunoreactivity in the sulcular epithelium (arrow in a2). (B) On day 7, immunoreactivity was greatly enhanced in the attached gingiva (star in b1), with subepithelial inflammation (arrowhead in b1 indicates the numerous infiltrating inflammatory cells in the subepithelial connective tissue). (C) On day 15, immunoreactivity was similar to that seen in the healthy state in the attached gingival epithelium (star in c1) and free gingival epithelium (filled circle in c2), whereas it was increased in the proliferative sulcular epithelium (arrow in c2). Phosphate-buffered saline was substituted for anti-EMMPRIN as a negative control and did not stain (A1–C1). Scale bars represent 200 μm.

osteoblasts were seen in the interradicular bone of healthy rats. Less information was provided for the role of EMMPRIN in physical alveolar bone remodeling. The role of bone-related EMMPRIN in periodontitis is of great interest and will be investigated further in future studies.

We previously demonstrated the distribution of EMMPRIN in human gingival epithelium. The immunoreactivity for EMMPRIN was strong in the basal layer cells and lessened toward the upper layers in healthy subjects, and was more widespead and more intense in periodontitis (7). In this study, we examined the temporal distribution of EMMPIN in rat gingival epithelium during the development of periodontitis and described it in three locations: the attached gingival epithelium, the free gingival epithelium and the sulcular epithelium. The distribution pattern in the attached gingival epithelium was similar to that in the human gingival epithelium. In addition, besides the basal layer cells, EMMPRIN was strongly expressed by the sulcular epithelial cells, which were invisible or hard to distinguish in resected human gingival tissue. The basal layer cells and the sulcular epithelial cells are both cell types with high turnover rates. The strong immunoreactivity in these cells indicated a possible connection of EMMPRIN with epithelial metabolism and renewal. The epithelium-derived EMMPRIN might also interact with connective tissue, because it markly increased with the aggravation of subepithelial inflammation.

Additionally, EMMPRIN was intensely expressed by the odontoblasts in the pulp. This was previously reported in a study on the role of EMMPRIN in tooth development (24). Positive staining was also observed in vascular endothelial cells, as we reported in a previous study (7). These immunostaining results did not obviously change during the observed period, and are therefore not shown.

To sum up, EMMPRIN was widely distributed in the rat periodontal tissues, and its expression and localization were temporally varied at different periods during the experimental periodontitis. Despite descriptive research, this study indicates that the roles of EMMPRIN during periodontitis should be considered in different cell types and at different stages of pathology. The inflammation-dependent expression of EMMPRIN is associated with alveolar bone loss and collagen breakdown. The epithelium-derived and the bone-related expression of EMMPRIN could also be involved in the pathogenesis of periodontitis, but warrant further in-depth studies.

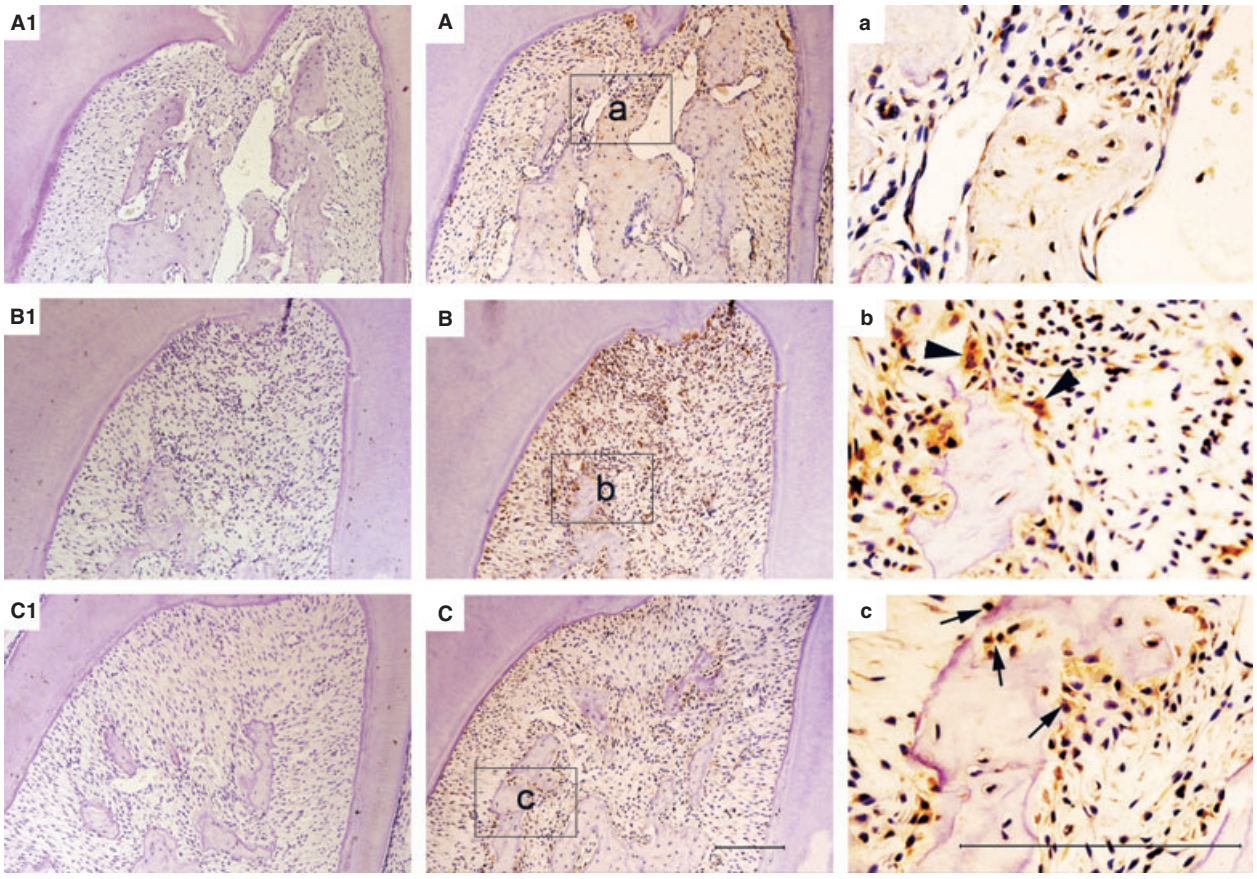

Fig. 5. Temporal expression and localization of EMMPRIN in the interradicular region. The immunoreactivity for EMMPRIN was weak in a few cells on day 0 (A,a); sharply increased in infiltraing cells and osteoclasts on day 7 (B,b); and present in numerous osteoblasts on day 11 (C,c). Arrowheads in (b) indicate the multinuclear osteoclasts in bone lacunas; arrows in (c) indicate the square-shaped active osteoblasts lining the bone surface. Positive staining could be seen in cementoclasts in cement lacunas and cementoblasts lining cement as well, in (B) and (C), respectively. Phosphate-buffered saline was substituted for anti-EMMPRIN as a negative control and did not stain (A1–C1). Scale bars represent 200 μm.

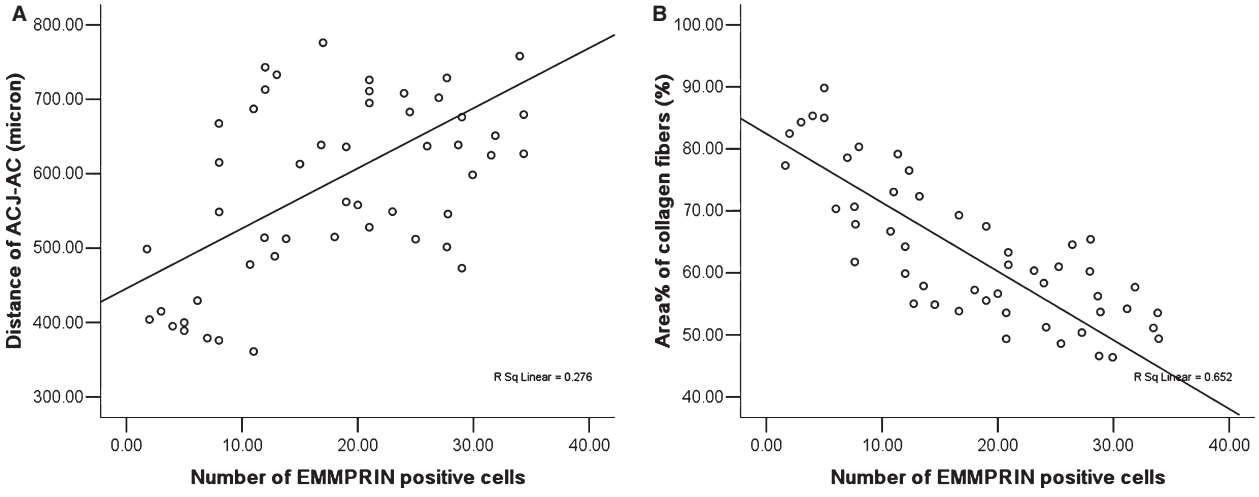

Fig. 6. Correlation analyses revealed a moderate positive correlation between EMMPRIN expression and the ACJ–AC distance ($r = 0.552$, $p = 0.002$; A), and a strong negative correlation between EMMPRIN expression with the Area% of collagen fibers ($r = -0.808$, $p = 0.000$; B).

Acknowledgements

The study has been supported by grants from the National Natural Science Foundation Emphases Item of China (30973313).

References

1. Page RC, Offenbacher S, Schroeder HE, Seymour GJ, Kornman KS. Advances in the pathogenesis of periodontitis: summary of developments, clinical implications and future directions. *Periodontol 2000* 1997;**14:**216–248.
2. Birkedal-Hansen H. Role of matrix metalloproteinases in human periodontal disease. *J Periodontol* 1993;**64:**474–484.
3. Nabeshima K, Iwasaki H, Koga K, Hojo H, Suzumiya J, Kikuchi M. Emmprin (basigin/CD147): matrix metalloproteinase modulator and multifunctional cell recognition molecule that plays a critical role in cancer progression. *Pathol Int* 2006; **56**(3)**:**359–367.
4. Yurchenko V, Constant S, Bukrinsky M. Dealing with the family: CD147 interactions with cyclophilins. *Immunology* 2006; **117**(3)**:**301–309.
5. Damsker JM, Okwumabua I, Pushkarsky T, Arora K, Bukrinsky MI, Constant SL. Targeting the chemotactic function of CD147 reduces collagen-induced arthritis. *Immunology* 2009;**126**(1)**:**55–62.
6. Emingil G, Tervahartiala T, Mantyla P *et al*. Gingival crevicular fluid matrix metalloproteinase (MMP)-7, extracellular MMP inducer, and tissue inhibitor of MMP-1 levels in periodontal disease. *J Periodontol* 2006;**77**(12)**:**2040–2050.
7. Cao Z, Xiang J, Li C. A potential role of EMMPRIN by regulating ECM degradation in periodontitis. *Med Hypotheses* 2007;**69**(5)**:**1102–1104.
8. Dong W, Xiang J, Li C, Cao Z, Huang Z. Increased expression of extracellular matrix metalloproteinase inducer is associated with matrix metalloproteinase-1 and -2 in gingival tissues from patients with periodontitis. *J Periodontal Res* 2009; **44**(1)**:**125–132.
9. Rovin S, Costich ER, Gordon AH. The influence of bacteria and irritation in the initiation of periodontal disease in germ-free and conventional rats. *J Periodontal Res* 1966;**1**(3)**:**193–204.
10. Page RC, Schroeder HE. Pathogenesis of inflammatory periodontal disease. A summary of current work. *Lab Invest* 1976; **34**(3)**:**235–249.
11. Heijl L, Rifkin BR, Zander HA. Conversion of chronic gingivitis to periodontitis in squirrel monkeys. *J Periodontol* 1976; **47:**710–716.
12. Schroeder HE, Lindhe J. Conversion of stable established gingivitis in the dog into destructive periodontitis. *Arch Oral Biol* 1975;**20**(12)**:**775–782.
13. Cai X, Li C, Du G, Cao Z. Protective effects of baicalin on ligature-induced periodontitis in rats. *J Periodontal Res* 2008; **43**(1)**:**14–21.
14. Junqueira LC, Bignolas G, Brentani RR. Picrosirius staining plus polarization microscopy, a specific method for collagen detection in tissue sections. *Histochem J* 1979;**11**(4)**:**447–455.
15. Nabeshima K, Suzumiya J, Nagano M *et al*. Emmprin, a cell surface inducer of matrix metalloproteinases (MMPs), is expressed in T-cell lymphomas. *J Pathol* 2004; **202**(3)**:**341–351.
16. Ge H, Zhang JF, Guo BS *et al*. Resveratrol inhibits macrophage expression of EMMPRIN by activating PPARgamma. *Vascul Pharmacol* 2007;**46**(2)**:**114–121.
17. Major TC, Liang L, Lu X, Rosebury W, Bocan TM. Extracellular matrix metalloproteinase inducer(EMMPRIN) is induced upon monocyte differentiation and is expressed in human atheroma. *Arterioscler Thromb Vasc Biol* 2002;**22**(7)**:**1200–1207.
18. Lim M, Martinez T, Jablons D *et al*. Tumor-derived EMMPRIN (extracellular matrix metalloproteinase inducer) stimulates collagenase transcription through MAPK p38. *FEBS Lett* 1998;**441**(1)**:** 88–92.
19. Taylor PM, Woodfield RJ, Hodgkin MN *et al*. Breast cancer cell derived EMMPRIN stimulates fibroblast MMP2 release through a phospholipase A(2) and 5-lipoxygenase catalyzed pathway. *Oncogene* 2002;**21**(37)**:**5765–5772.
20. Si AI, Huang L, Xu J, Kumta SM, Wood D, Zheng MH. Expression and localization of extracellular matrix metalloproteinase inducer in giant cell tumor of bone. *J Cell Biochem* 2003; **89**(6)**:**1154–1163.
21. Gabison EE, Mourah S, Steinfels E *et al*. Differential Expression of extracellular matrix metalloproteinase inducer (CD147) in normal and ulcerated corneas. *Am J Pathol* 2005;**166**(1)**:**209–218.
22. Menashi S, Serova M, Ma L, Vignot S, Mourah S, Calvo F. Regulation of extracellular matrix metalloproteinase inducer and matrix metalloproteinase expression by amphiregulin in transformed human breast epithelial cells. *Cancer Res* 2003; **63**(22)**:**7575–7580.
23. Schwartz Z, Goultschin J, Dean DD, Boyan BD. Mechanisms of alveolar bone destruction in periodontitis. *Periodontol 2000* 1997;**14:**158–172.
24. Schwab W, Harada H, Goetz W *et al*. Immunocytochemical and biochemical detection of EMMPRIN in the rat tooth germ: differentiation-dependent co-expression with MMPs and co-localization with caveolin-1 in membrane rafts of dental epithelial cells. *Histochem Cell Biol* 2007;**128**(3)**:**195–203.